Analysis of diffraction efficiency of phase gratings in dependence of duty cycle and depth

A.Yu. Meshalkin[1], V.V. Podlipnov[2,3], A.V. Ustinov[3], E.A. Achimova[1]

[1]Institute of Applied Physics, Academiei str. 5, MD-2028, Chisinau, Moldova
[2]Samara National Research University, Moskovskoe Shosse 34, Samara, Russia, 443086
[3]Image Processing Systems Institute of RAS - Branch of the FSRC "Crystallography and Photonics" RAS, Molodogvardejskaya street 151, Samara, Russia, 443001

Abstract. The analysis of dependence of diffraction efficiency on duty cycle and modulation depth of phase gratings with rectangular and Gaussian profile was performed by means of specially designed program. An Angular Spectrum method applied for monochromatic light propagation in far field through phase grating was used for calculation of diffraction efficiency of gratings. Diffraction efficiency maps of 0-5th diffraction orders were obtained for different grating profiles. It is shown that changing the duty cycle of grating makes it possible to tune smoothly the diffraction efficiency and to redirect the light intensity in required orders.

1. Introduction

Diffraction gratings are commonly used as dispersive elements in many optical systems. Applications include spectrometers, switching, tuning and trimming elements in dense wavelength-division multiplexing, visual display technology, external cavity lasers, etc. [1-3]. The diffraction efficiency of grating is an important parameter since it will strongly influence the final energy delivered by the optical diffraction system. High diffraction efficiency can be very challenging to achieve at the necessary spectral bandwidth in selected diffraction order [4-6]. To address these different challenges, several types of diffraction gratings can be used related either to the manufacturing process (ruled gratings, holographic gratings, master gratings, replica gratings), the nature of the modulation (surface relief gratings, volume gratings, amplitude gratings), or the optical configuration (transmission gratings, reflection gratings) [7].

The theoretical analysis of diffraction gratings is classically derived within the theory of scalar optics [9]. The diffraction grating is composed by a series of parallel and periodic ridges formed on the appropriate material [9]. The intensities of different diffraction orders can be analyzed by means of the Kirchhoff diffraction theory considering each ridge as a secondary source of radiation. By applying the Fraunhofer approximation, the discrete diffractive orders are given by the constructive interference position between the waves emitted by each source [10]. The diffracted intensity results from the product between the intensity function of a single ridge and the interference function. It classically features sharp peaks due to the interference function modulated by the intensity function. The former depends on the grating period while the latter depends on the geometry of the ridge [11,12]. However, as it is noted in [13], this simplified approach does not explain the relative intensities of the diffracted orders of a diffraction grating, because the diffraction envelope associated with the ridge shape and its width is ignored. Diffraction gratings with ridge width being half of the

period are more common, but other relationships between period and ridge width are possible [14]. The effect of this envelope function is so important that some diffraction orders may disappear, although they fulfil the above-mentioned interference condition. For instance, the simplest binary diffraction grating, where the width of the ridge is equal to the half of the grating period, produces a diffraction pattern where all even diffraction orders are missing [15]. For optical processing and switching, the intensity ratio of the diffracted and main beams of the grating needs to be controlled to within a certain range. This ratio can be affected by the variation of duty cycle and phase depth.

In this work, we present an evaluation the diffracted order intensities of binary phase diffraction gratings with different duty cycles (defined as the ratio of the grating ridge width to the grating period) and ridge heights (depth of phase modulation). This method is based on Angular Spectrum method applied for monochromatic light propagation through phase grating. Both the duty cycle and ridge height value were taken in account since they are directly related to the diffraction order intensity. The proposed method allows the calculation of the intensity of the particular diffraction orders for both amplitude and phase gratings with arbitrary profile.

2. Modelling of light diffraction by Angular Spectrum method

Scalar approximations of phase or amplitude diffraction gratings can be derived on the basis of an electromagnetic theory starting with the Maxwell differential equations, while these can be developed into the methods of modern Fourier optics. In the object and image plane, small patches surrounding the analyzed point were considered and associate them with the Fourier expansion, a superposition of plane waves [16]. The concept of intensity is tightly related to space-frequency distribution in the prediction of the phase morphology of microstructures. It was shown in [17] that free propagation of light with imaging of diffraction pattern can be modeled with good accuracy by computing the propagation of a complex wave, which can be done using several approximations [18]. For simulating of the diffraction process we applied Angular Spectrum method (ASM) [19] that involves expanding a complex wave into a summation of infinite number of plane waves, and is suitable for both near and far field of diffraction [20]. In far field the ASM method recovers Fraunhofer diffraction that is used for diffraction efficiency analyses.

Let us suppose the coherent light is being transmitted through the phase diffraction grating. Monochromatic beam of the plane waves falls normally to the grating.

The angular spectrum of the diffracted light $F_0(k_x,k_y)$ is described by the expression:

$$F_0(k_x, k_y) = \frac{1}{(2\pi)^2} \int \int_{-\infty}^{\infty} u_0(x, y, 0) \exp[-\mathrm{i}(k_x x + k_y y)] \, \mathrm{d}x \, \mathrm{d}y. \quad (1)$$

The complex amplitude of the wave in the plane z=0 is described by the function $u_0(x,y,0)$.

In fact, in the plane z=0 the integrand of (1) expresses the complex amplitude of the plane harmonious wave with the components of the wave vector k_x, k_y and k_z

$$k_z = \sqrt{k^2 - k_x^2 - k_y^2} \quad (2)$$

The complex spectrum $F_0(k_x,k_y)$ depends upon the distribution of direction (time-term multiplier $\exp(-i\omega t)$ is omitted). Variables $k_x = k\cos\alpha$, $k_y = k\cos\beta$, $k_z = k\cos\varphi$, where $\cos\alpha$, $\cos\beta$, $\cos\varphi$ are the direction cosines of the wavefront normal and $k=2\pi/\lambda$ is the wave number. The initial distortion of the angular spectrum depends upon the range of k_x and k_y, the width of the angular spectrum $F_0(k_x, k_y)$ in the plane z=0. The transmission characteristic of the grating T(x,y) was introduced. Every particular grating is characterized by its own T(x,y).

If we define the field of the falling wave in the plane z=0 as $u_f(x,y)$, then the field behind the grating is defined by the formula $u_0(x;y;0)=u_f(x;y)*T(x,y)$ and the angular spectrum behind the grating is equal to the convolution of the angular spectrum of the falling field and the spectrum of the transmission grating.

In the case of phase grating diffraction, shown in Fig. 1., the grating characteristic function T(x,y) is equal to $T(x,y)=A_0\exp(i\Delta\varphi(x,y))$, where A_0 – is constant amplitude, and $\Delta\varphi(x,y)$ – is light phase modulation induced by grating. Diffraction pattern from phase grating, that produces specified light

phase modulation was obtained by AS in the case of unit amplitude (A0=1) and distance z=10mm>>λ (far field diffraction). The intensity of each diffraction order I_m was collected and the diffraction efficiency was calculated by $\eta_m=I_m/I_0*100\%$, where $I_0=A_0^2$ – is the intensity of incident light, m – diffraction order. In our simulation we used λ=650 nm.

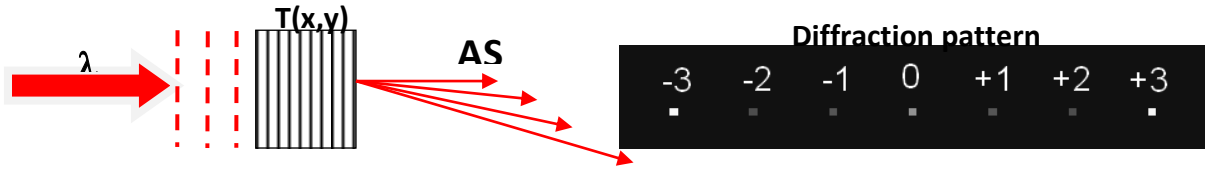

Figure 1. Diffraction on phase grating described by function T(x,y) and imaging of diffraction pattern using AS.

3. Diffraction from phase grating with rectangular profile

The schematic of a diffraction from phase grating with rectangular profile is shown in Fig. 2, where *a* is ridge width, *b* is grating period, and *h* is relief depth. The grating duty cycle parameter (D) is defined as the ratio of the grating ridge width to the period D=a/b*100%. The grating period was considered of being constant with value of 5 μm, while the ridge with was varied from 0 μm to 5 μm resulting in D variation from 0% up to 100%.

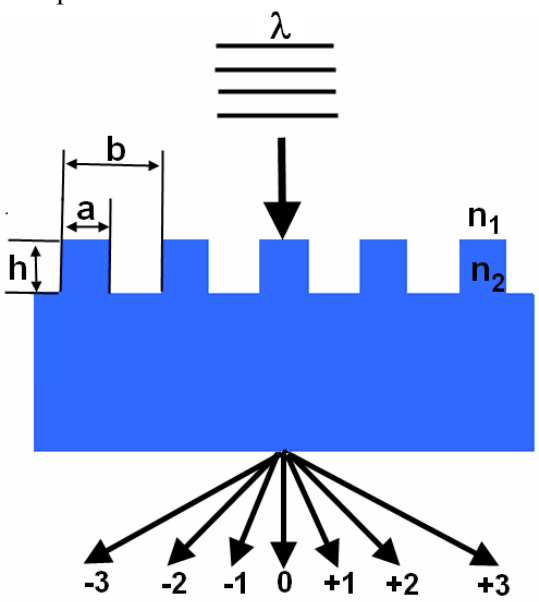

Figure 2. Schematic representation of light diffraction from phase grating with rectangular profile (λ - wavelength of incident plane wave, n_1 and n_2 – refractive indexes of surrounding media and grating correspondingly, a - bridge width; b – grating period, h – grating depth, −3, -2, …, +3 – corresponding diffraction orders).

A plane wave illuminates the grating under normal incidence. The phase of light that is passed through such grating is modulated according to the grating profiley Δφ(x,y)~h(x,y). The amplitude of phase modulation Δφ induced by surface relief grating can be expressed as $\Delta\varphi=2\pi/\lambda(h\cdot(n_2-1))$ (3), and by refractive index grating as $\Delta\varphi=2\pi/\lambda(d\cdot\Delta n)$ (4), where λ is the light wavelength, h – surface modulation depth, n_2 – refractive index of grating material, d – film thickness, Δn – amplitude of refractive index modulation [9]. A duty cycle parameter was varied from 0% to 100% by step 1%.

Diffraction efficiency for gratings with an arbitrary profile may be calculated analytically by Fourier series expansion [21]. For gratings with rectangular profile, diffraction efficiency is expressed by simple formula:

$$\eta_0 = 1-2D+2D^2+2D(1-D)\cos(\Delta\varphi),$$
$$\eta_m = \frac{4}{\pi^2 m^2}\sin^2(\pi m D)\sin^2(\Delta\varphi/2). \quad (4)$$

Particularly, if D=0.5 we get from Eq. (4):

$$\eta_0 = \cos^2(\Delta\varphi/2),$$
$$\eta_m = \frac{4}{\pi^2 m^2}\sin^2(\pi m/2)\sin^2(\Delta\varphi/2). \quad (5)$$

Also, if $\Delta\varphi = \pi$ we get:

$$\eta_0 = (1-2D)^2,$$
$$\eta_m = \frac{4}{\pi^2 m^2}\sin^2(\pi m D). \quad (6)$$

The diffraction efficiency coupled into the diffraction orders 0-6 for grating with D=50% in dependence on amplitude of phase modulation Δφ (0-2π rad) is presented in Fig. 3.

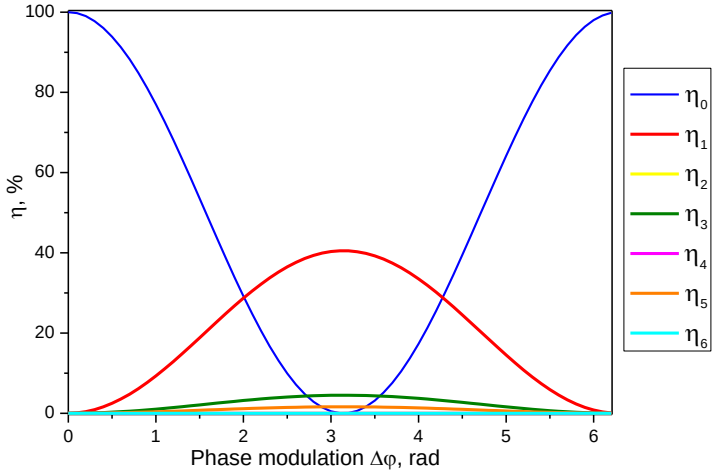

Figure 3. The dependences of diffraction efficiency of grating with D=50% on amplitude of phase modulation Δφ obtained for 0-6 diffraction orders.

As it is seen such grating produces a diffraction pattern where all even diffraction orders are missing and the obtained maximum value of first order diffraction efficiency is equal to 40.5% at phase modulation Δφ=π rad. The maximum value of 3-rd order diffraction efficiency is about 4.5% at the same phase depth.

Diffraction efficiency for 0-5th orders (η_0-η_5) of the rectangular profile grating in dependence of duty cycle (D=0÷100%) and phase depth (Δφ=0÷2π rad) is presented in Fig. 4.

The dependence of diffraction efficiency on duty cycle at phase depth Δφ=π rad is presented in Fig. 5.

The second order diffraction efficiency increases up to 10.1% at D=25% and D=75%, while η_3 reaches the same value of 4.5% at D=16.7%, D=50.0% and D=83.3%. In the cases of D=33% and 66% the third order diffraction is missing. In the cases of D=25%, 50% and 75% the 4-th order diffraction is missing. The 5-th order diffraction is missing in the cases of D=20%, 40%, 60% and 80%. Therefore, changing the duty cycle of grating makes it possible to tune smoothly the diffraction efficiency in each order and to redirect the light intensity in required orders.

4. Diffraction from phase grating with Gaussian profile

Diffraction gratings that modulate the phase rather than the amplitude of the incident light are usually produced using laser holography or electron-beam lithography. Gaussian intensity (irradiance) profile describes the beam output of most lasers and e-beam sources. Profile of each Gaussian ridge was modelled as $h(x)=exp(-2e*x^2/a^2)$, where a defines width of the Gaussian ridge, e is base of the natural

logarithm, and *x* was varied in interval [-1,1]. The phase of light that is passed through such grating is modulated according to the surface topography $\Delta\varphi(x,y)=2\pi/\lambda(h(x,y)\cdot(n_2-1))$. The duty cycle D of such grating is defined as the ratio of the grating ridge width *a* to the double distance between adjacent Gaussian ridges *b,* D=a/2b·100%. Profiles of grating with different D are shown in Fig. 6.

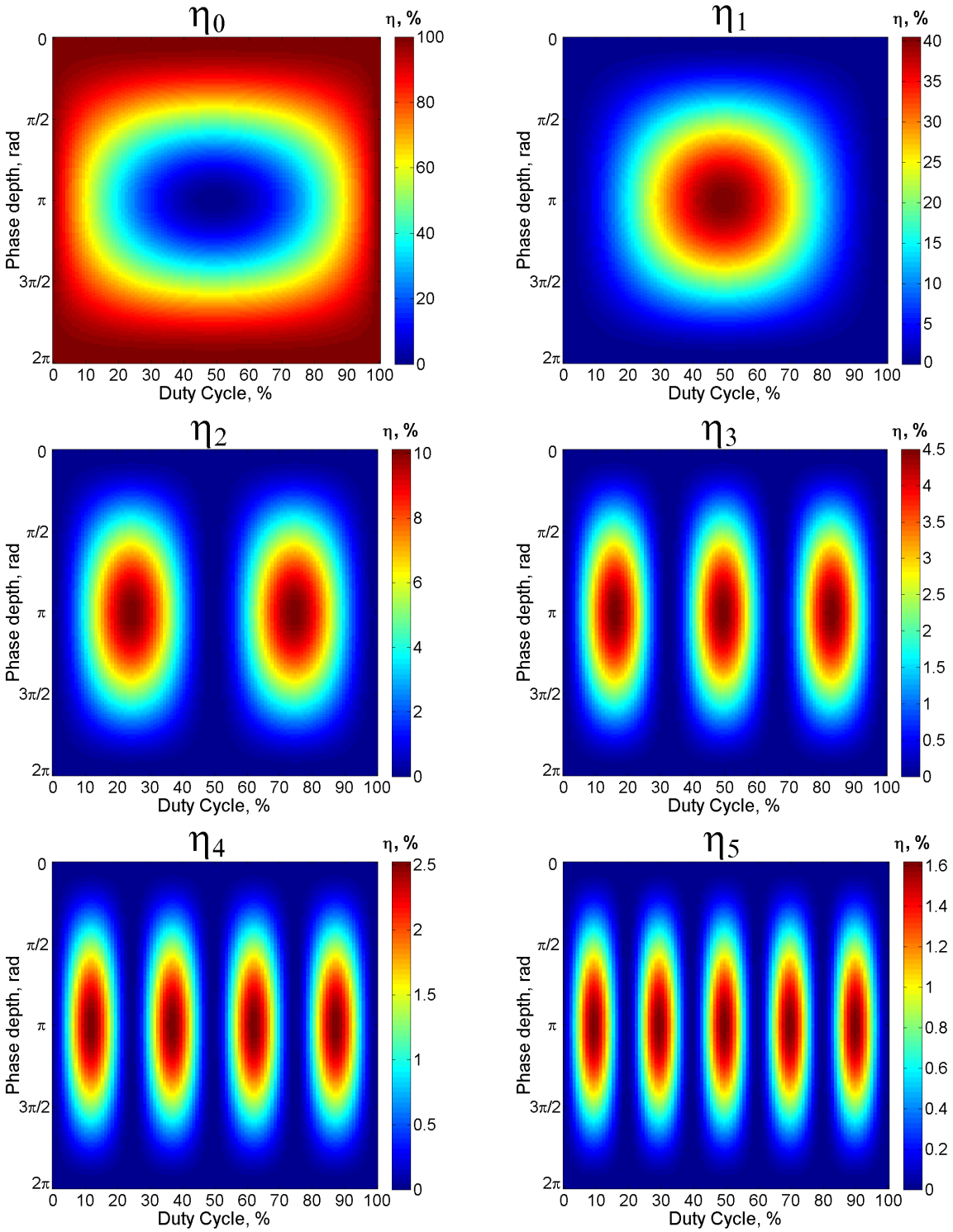

Figure 4. Map of diffraction efficiencies (η_0-η_5) of the rectangular profile grating versus duty cycle and phase depth. Color map corresponds to diffraction efficiency.

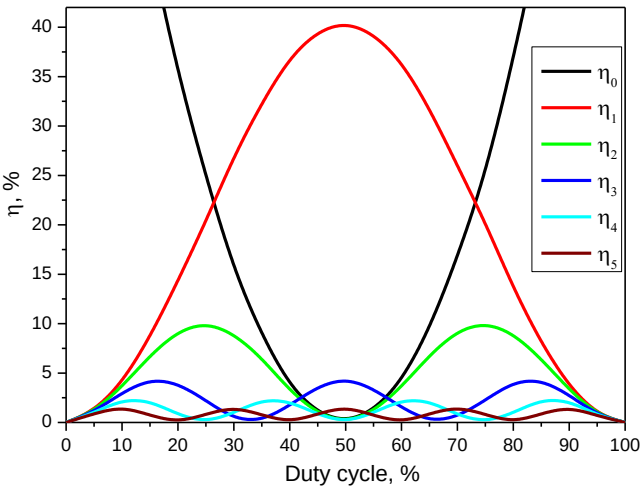

Figure 5. Dependence of diffraction efficiency on duty cycle at phase depth Δφ=π rad.

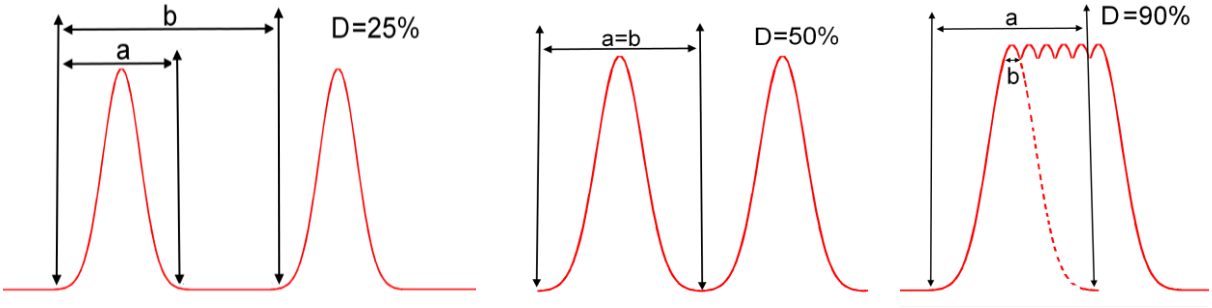

a) b) c)

Figure 6. Profiles of gratings with Gaussian shape of ridge and different duty cycle: *a* – 25%, *b* – 50%, *c* – 90%.

The diffraction efficiency coupled into the 0-5th diffraction orders for grating with Gaussian ridge profile and D=50% in dependence on amplitude of phase modulation Δφ (0-5π rad) is presented in Fig. 7a. For comparing the similar dependencies of diffraction efficiencies $\eta_0 \ldots \eta_5$ of grating with sinusoidal profile are presented in Fig. 7b.

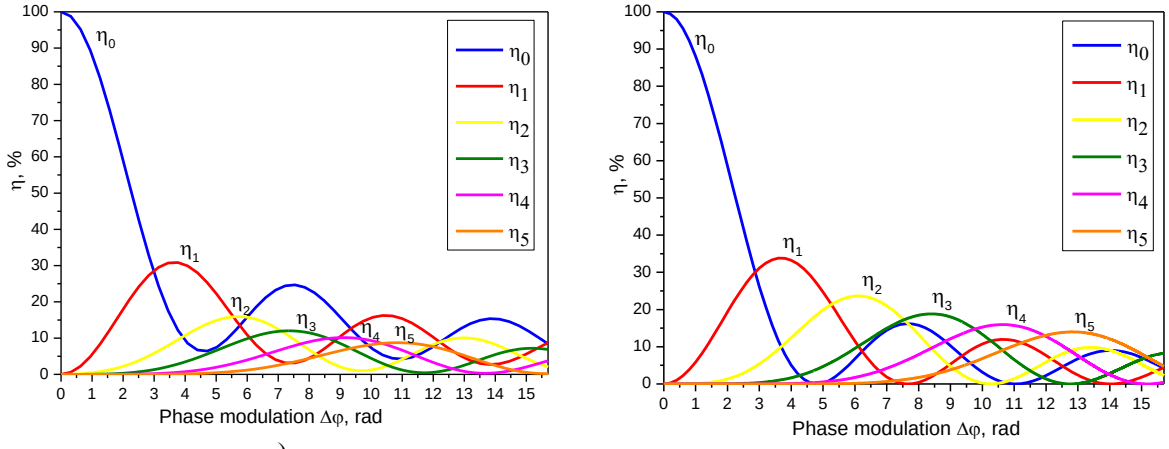

a) b)

Figure 7. Dependences of diffraction efficiencies $\eta_0 \ldots \eta_5$ on phase modulation Δφ for Gaussian bridge profile (a) and sinusoidal one (b).

As it is seen from the Fig. 7, the kinetics of diffraction efficiency of grating with Gaussian bridge profile looks like one of sinusoidal grating. For sinusoidal grating the diffraction efficiency of m diffraction

order η_m is described by Bessel function of the first kind, $\eta_m=J_m^2(\Delta\varphi/2)$ [22], where $\Delta\varphi$ is amplitude of phase modulation (Fig. 7b). The maximum diffraction efficiency is observed for first diffraction order and it is equal to 33.8% at phase modulation $\Delta\varphi=3.6$ rad. The dependence $\eta_m(\Delta\varphi)$ of each diffracted order has alternate peaks and minimum values of 0%. Except for the zero diffracted order diffraction efficiencies of all diffraction orders have smaller values for Gaussian profile of bridge, than for sinusoidal one. The maximum value of η_1 is about 30% (for Gaussian shape grating), while for sinusoidal one it is about 33.8%. It is obvious that grating with Gaussian profile and D=50% doesn't correspond to sinusoidal grating (Fig. 8a). Varying the duty cycle of grating with Gaussian grating profile, it is possible to obtain the grating profile close to sinusoidal one (at D=62.5%), that can be seen in the Fig. 8b.

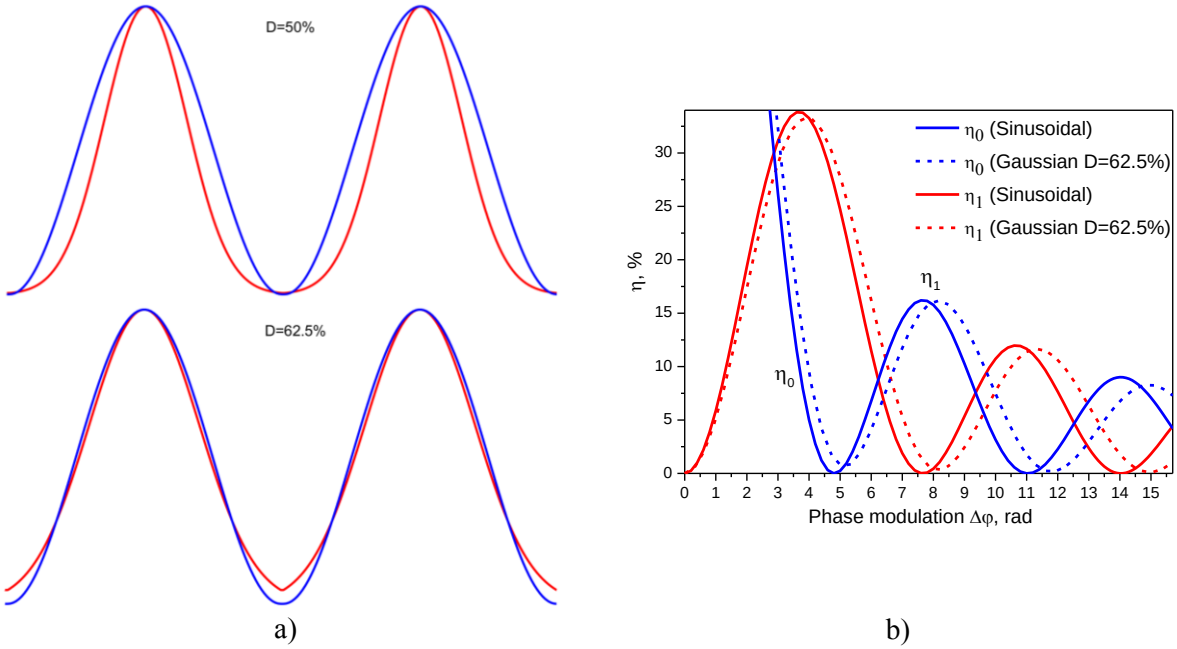

a) b)

Figure 8. a - Profile of gratings (Sinusoidal – blue curve, Gaussian – red curve) with D=50% and D=62.5% for Gaussian bridge profile; b - Dependences of diffraction efficiency on $\Delta\varphi$ ($\Delta\varphi$ =0-5π rad) for Gaussian bridge profile with D=62.5% and sinusoidal one.

Dependences of 0-5th orders diffraction efficiencies $\eta_0 \ldots \eta_5$ of Gaussian profile grating on phase depth ($\Delta\varphi=0\div5\pi$ rad) are shown in Fig. 9.

As can be seen from Fig. 9, the phase grating with Gaussian bridge profile has considerably different diffraction efficiency map compared with rectangular profile grating (Fig. 4). In Fig. 4 the dependence of diffraction efficiency on duty cycle is symmetrical relative to varying of D, while the same dependence of diffraction efficiency for Gaussian profile grating is asymmetrical. Maximum value of diffraction efficiency shifts to higher value of duty cycle due to two reasons: (i) profile of grating with higher duty cycle value is close to sinusoidal one (at D=62.5%), (ii) phase depth of grating with D>50% starts to decrease due to intersecting of adjacent bridges. Therefore the optimization of grating parameters, such as the phase depth and the duty cycle, could be done to obtain the maximum value of diffraction efficiency of required diffracted order.

5. Conclusions

The analysis of diffraction efficiency on duty cycle and light modulation induced by phase gratings with rectangular and Gaussian profile is described. Diffraction efficiency maps of 0-5th diffraction orders were obtained for each type of grating profile. It was established missing of some diffraction orders for certain duty cycles of gratings with rectangular profile. The dependence of the diffraction efficiency on duty cycle is symmetrical relative to varying of duty cycle value for the grating with rectangular profile, while the same dependence of diffraction efficiency for grating with Gaussian

profile is asymmetrical: maximum diffraction efficiency value shifts to higher values of duty cycle and reaches peak value at D=62.5%. At this value the profile of grating is close to sinusoidal. Changing the duty cycle of grating makes it possible to tune smoothly the diffraction efficiency and to redirect the light intensity in required diffracted orders.

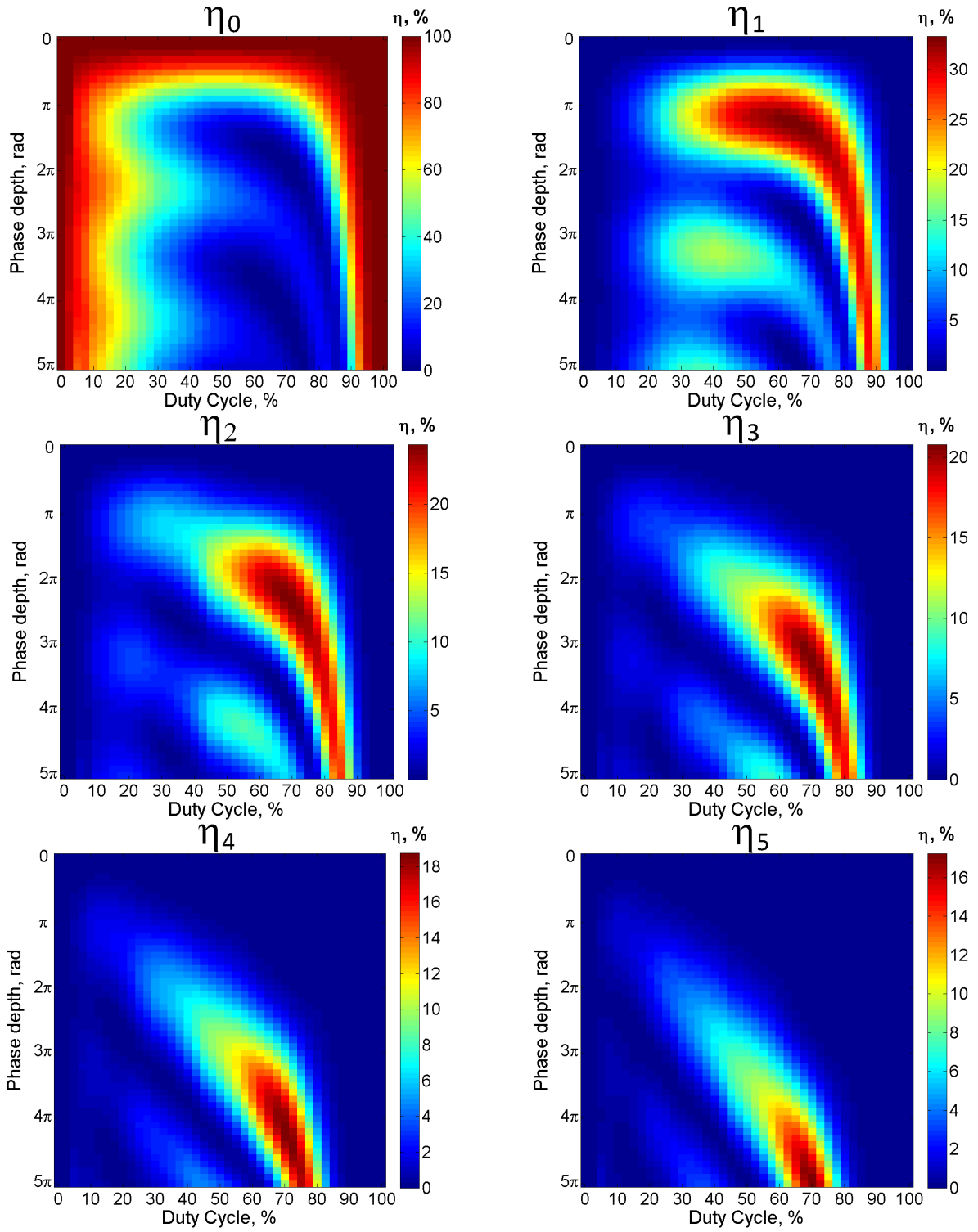

Figure 9. Dependences of diffraction efficiency of the phase grating with Gaussian profile on duty cycle and phase depth. Color map corresponds to diffraction efficiency.

6. References

[1] Bonod, N. Diffraction gratings: from principles to applications in high-intensity lasers / N. Bonod, J. Neauport // Adv. Opt. Photon. – 2016. – Vol. 8. – P.156-199.

[2] Alonso-Ramos, C. Polarization-independent grating coupler for micrometric silicon rib waveguides / C. Alonso-Ramos, L. Zavargo-Peche, A. Ortega-Moñux, R. Halir, I. Molina-Fernández, P. Cheben // Opt. Lett. – 2012. – Vol. 37(17). – P. 3663-3665.

[3] Feng, J. Three-port beam splitter of a binary fused-silica grating / J. Feng, C. Zhou, B. Wang, J. Zheng, W. Jia, H. Cao, P. Lv // Appl. Opt. – 2008. – Vol. 47. – P. 6638-6643.

[4] Rathgen, H. Large bandwidth, highly efficient optical gratings through high index materials / H. Rathgen, H.L. Offerhaus // Opt. Express. – 2009. – Vol. 17. – P. 4268-4283.

[5] Doskolovich, L.L. Design and investigation of color separation diffraction gratings / L.L. Doskolovich, N.L. Kazanskiy, S.N. Khonina, R.V. Skidanov, N. Heikkilä, S. Siitonen, J. Turunen // Appl. Opt. – 2007. – Vol. 46(15). – P. 2825-2830.

[6] Karpeev, S.V. Study of the diffraction grating on the convex surface as a dispersive element / S.V. Karpeev, S.N. Khonina, S.I. Kharitonov // Computer Optics. – 2015. – Vol. 39(2). – P. 211-217.

[7] Palmer, C. Diffraction Grating Handbook / C. Palmer. – New York: Newport Corporation, 2014. – 265 p.

[8] Andries, I. Approximate analysis of the diffraction efficiency of transmission phase holographic gratings with smooth non-sinusoidal relief / I. Andries, T. Galstian, A. Chirita // J. Optoel. Adv. Mater. – 2016. – Vol. 18. – P. 56-64.

[9] Cazac, V. Surface relief and refractive index gratings patterned in chalcogenide glasses and studied by off-axis digital holography / V. Cazac, A. Meshalkin, E. Achimova, V. Abashkin, V. Katkovnik, I. Shevkunov, D. Claus, G. Pedrini //Appl. Opt. – 2018. – Vol. 57. – P. 507-513.

[10] Duffieux, P.M. The Fourier Transform and its Applications to Optics / P.M. Duffieux. – New York: Wiley, 1983. – 217 p.

[11] Ustinov, A.V. Effect of the fill factor of an annular diffraction grating on the energy distribution in the focal plane / A.V. Ustinov, A.P. Porfir'ev, S.N. Khonina // J. Opt. Technol. – 2017. – Vol. 84. – P. 580-587.

[12] Khonina, S.N. Diffractive axicon with tunable fill factor for focal ring splitting / S.N. Khonina, A.P. Porfirev, A.V. Ustinov // Proc. SPIE. – 2017. – Vol. 10233. – P. 102331P.

[13] Mezouari, S. Validity of Fresnel and Fraunhofer approximations in scalar diffraction / S. Mezouari, A.R. Harvey // J. Opt. A: Pure Appl. Opt. – 2003. – Vol. 5(4). – P. S86-S91.

[14] Torcal-Milla, F.J. Diffraction by gratings with random fill factor / F.J. Torcal-Milla, L.M. Sanchez-Brea // Appl. Opt. – 2017. – Vol. 56. – P. 5253-5257.

[15] Shih, W.-C. High-resolution electrostatic analog tunable grating with a single-mask fabrication process / W.-C. Shih, S.-G. Kim, G. Barbastathis // J. Microelectromech. S. – 2006. – Vol. 15(4). – P. 763-769.

[16] Comastri, S.A. Generalized sine condition for image-forming systems with centering errors / S.A. Comastri, J.M. Simon, R. Blendowske // J. Opt. Soc. Am. A. – 1999. – Vol. 16(3). – P. 602-612.

[17] Matsushima, K. Band-limited angular spectrum method for numerical simulation of free-space propagation in far and near fields / K. Matsushima, T. Shimobaba // Opt. Express. – 2009. – Vol. 17. – P. 19662-19673.

[18] Kreis, T.M. Methods of digital holography: A comparison / T.M. Kreis, M. Adams, W.P.O. Juptner // Proc. SPIE. – 1997. – Vol. 3098. – P. 224-233.

[19] Shimobaba, T. Scaled angular spectrum method / T. Shimobaba, K. Matsushima, T. Kakue, N. Masuda, T. Ito // Opt. Lett. – 2012. – Vol. 37. – P. 4128-4130.

[20] Kozacki, T. Angular spectrum-based wave-propagation method with compact space bandwidth for large propagation distances / T. Kozacki, K. Falaggis // Opt. Lett. – 2015. – Vol. 40. – P. 3420-3423.

[21] Goodman, J.E. Introduction to Fourier Optics / J.E. Goodman. – New York: McGraw-Hill, 1996. – 464 p.

Acknowledgments
The authors would like to thank Dr. Sergei Sergeev for the helpful suggestions and article corrections. This research was partially supported by the H2020-TWINN-2015 HOLO project (nr. 687328), Russian Foundation for the Basic Research (Project No 18-29-20045-мк, Project No 16-29-09528 ofi-m, Project No. 18-07-01470).